

# Functionally Graded Copper – Steel Using Laser Engineered Net Shaping™ Process

Fredrick F. Noecker II and John N. DuPont

Department of Materials Science and Engineering, Lehigh University  
Bethlehem, PA 18015

## Abstract

Laser Engineered Net Shaping™ (LENS™) is an emerging Solid Freeform Fabrication (SFF) process capable of producing fully dense metallic parts with complex shapes directly from a computer-aided drawing (CAD) without the need for molding or tooling. The LENS™ process also shows promise in producing components with graded compositions. One potential application is the production of steel – copper die casting materials. Copper is currently deposited on dies made out of steel to enhance thermal management, however, difficulties can occur at the Fe-Cu interface, such as, a large solidification temperature range in the Fe-Cu system (which can cause solidification cracking), formation of undesirable phases, and differences in coefficient of thermal expansion. The current research goal is to develop LENS™ processing parameters to optimize the deposition of functionally graded steel - Copper alloy. Dilution control experiments were carried out to determine the cracking susceptibility of Steel - Cu alloys of varying compositions. The resulting microstructures were characterized by various microscopy techniques. The influence of composition on the resultant cracking susceptibility and microstructure will be discussed. This information is useful for successful deposition of crack-free copper layers onto steel for die casting applications.

(189 words in abstract)

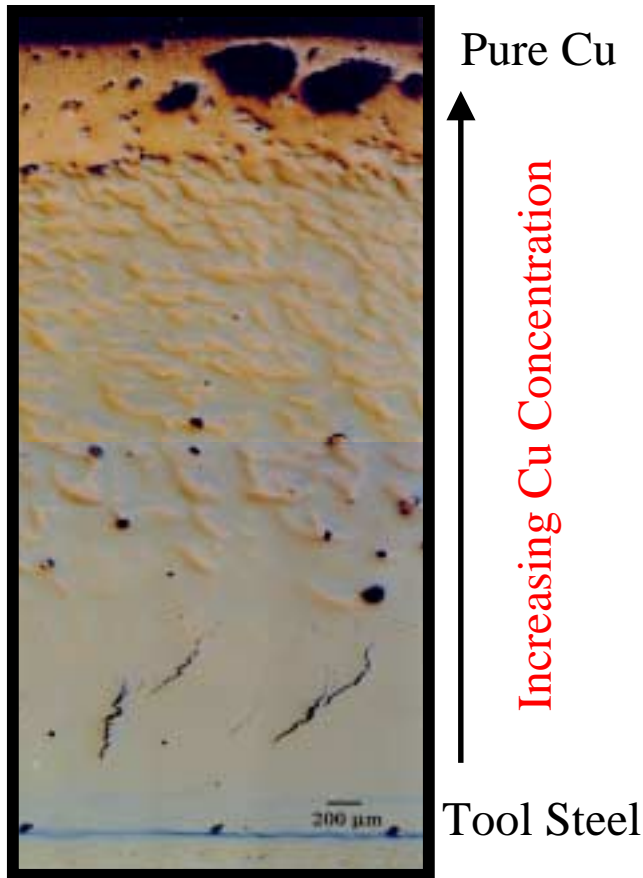
## Introduction

Laser Engineered Net Shaping™ (LENS™) is a growing solid free form fabrication process capable of producing fully dense 3-D complex shapes directly from a Computer Aided Design (CAD) drawing via Direct Metal Deposition (DMD). LENS utilizes an Nd-YAG laser to produce a melt pool on a substrate attached to an X-Y table. Powder metal from coaxial powder flow nozzles is injected into the melt pool as the table is moved along a pre-designed tool path thus producing a fully dense part by depositing line after line which become sequential layers. LENS has already proven its ability to produce molds with out of AISI H-13 Tool Steel (ref Mazumder 97) and shown promise in producing conformal cooling channels in molds made out of the same material (ref Knights 01). Additionally, several researchers have investigated the fabrication of functionally graded materials using direct metal deposition variant processes (ref Brice 00, Fessler 97, Li 99).

AISI H-13 tool steel is a widely used mold material due to its favorable mechanical properties, but the thermal conductivity limits the melt cooling rate and subsequent mold cycle time. The thermal conductivity of copper is nearly twice that of AISI H-13 tool steel at operating temperatures between 220-600 C (ref CarTech H-13 physical properties sheet, Touloukian 70).

Attempts have been made to clad materials with higher thermal conductivity, such as copper, to molds. This has resulted in limited success due to the difference in thermal coefficient of expansion between copper and steel, which creates larger thermal stresses at the clad interface ultimately resulting in failure. The tool and die industry would like to exploit the combined LENS capability of producing functionally graded materials and with conformable cooling channels to improve die thermal management which will subsequently increase productivity. By increasing productivity 20%, every fifth day of production is free, along with cascading manufacturing variables that can result in a marked increase in profits (ref. Beard 01)

Proof of Concept Experiment



The LENS was used to create a Functionally Graded Material (FGM) cube of H-13 tool steel and copper to evaluate metallurgical factors. Copper was continuously graded into H-13 tool steel that was deposited on a plain carbon steel substrate. Table 1 contains alloy compositional information. Figure 1 is an as polished light optical micrograph of the longitudinal cross-section revealing cracking and porosity. Porosity was observed in the FGM as the concentration of copper increased. The porosity is believed to be a function of the copper powder’s dendrite morphology. A spherical powder shape should provide the solution to the porosity problem.

**Figure 1:** FGM montage of H-13 – Copper LENS deposit

**Table 1 –** Composition of alloys used in steel – copper FGM and dilution control experiments

Cracking was also observed in the FGM in the region where copper gradient began. Copper has been shown by several researchers to promote solidification cracking/hot cracking in steel (ref Asnis 65, Vainerman 68, Cooper 74, Dixon 81). The susceptibility of steel – copper alloys to solidification cracking is evident in the Fe-Cu phase diagram, Figure 2 (Swartzendruber 90) which reveals a large solidification temperature range and very limited solid solubility of either element which will lead to large amounts of terminal liquid. Additionally, the dihedral angle for copper – mild steel is below 25° throughout the solidification temperature range, thus promoting austenite grain boundary wetting by copper (ref. Salter 66).

## Dilution Control Experimental Procedure

To avoid crack susceptible steel – copper concentrations, the range of copper concentration in steel that promote cracking must first be known. Dilution control experiments (ref DuPont 96) were undertaken to determine this compositional cracking range. Dilution experiments utilizing a Gas Tungsten Arc Welder (GTAW) with an automated cold wire feed provided an elegant way to easily produce a wide range of steel – copper compositions, knowing the filler metal and base metal compositions (see Table 1). Copper bead on rolled 1” wide x ¼” thick AISI 1013 steel

rolled bar welds were made with all weld processing parameters constant except wire feed speed. AISI 1013 steel was selected as a simplified, yet fairly representative system for AISI H-13 tool steel. Also, it is hoped that the results produced by welding copper onto steel under a condition of low restraint will be used in a broad range of applications beyond DMD.

The GTAW was set up with a .01” arc gap, 2mm/s travel speed, 250 amp current and 10 volt potential. The shielding gas was commercially pure Ar. The steel rolled bar was held along its entire length by a welding jig until the sample cooled to the touch. Volumetric filler metal feed rate is a function of wire feed speed, which was varied to alter the composition of copper in the fusion zone. Samples were fabricated with compositions ranging from AISI 1013 Steel 7 wt% Cu to 98 wt% Cu.

Weld transverse cross sections of each welding condition were sectioned, mounted, ground and polished using standard Metallographic techniques, then etched in 2% Nital. Digital stereograph images were taken of each sample and fusion zone measurements taken using Pax-It quantitative image analysis program. Geometric dilution measurements have shown good correlation, within  $\pm 2.6\%$  (ref. Banovic 01) to  $\pm 5\%$  (ref. DuPont 99) with Electron Probe Micro Analysis measurements.

## Results and Discussion

Table 2 summarizes the geometrically determined fusion zone composition of each sample in conjunction with visual and microscopic observations. In every instance copper was observed in the FZ, cracking was observed in the HAZ, most often along prior  $\gamma$  grain boundaries. The observations in Table 2 do not directly indicate a distinct composition range at which copper causes cracking the FZ of Steel – Cu welds, however, taking into account the margin of difference found by Banovic and DuPont, three regions of FZ crack susceptibility emerge: low, moderate and high. These regions are graphically shown in Figure 3.

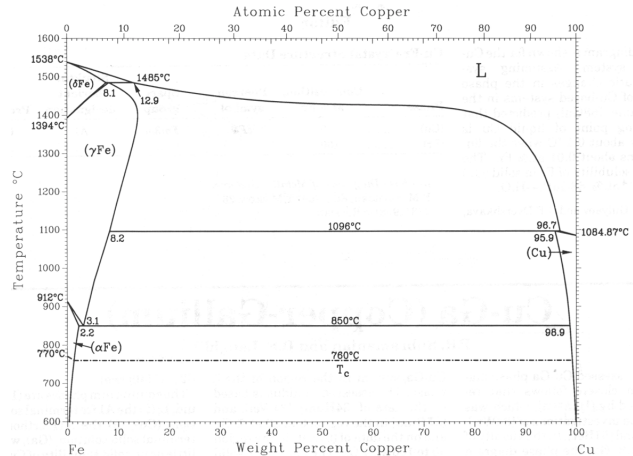


**Figure 2: Fe-Cu Phase Diagram**

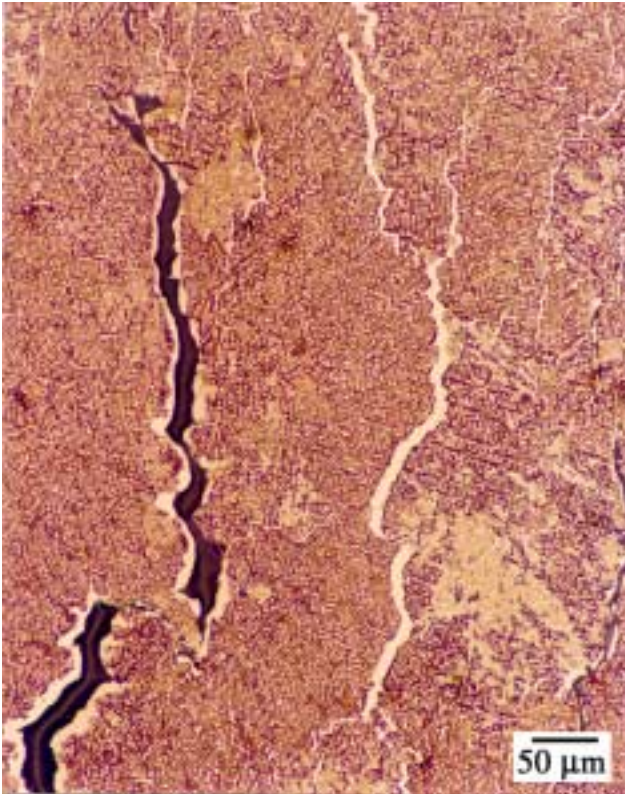


**Figure 6:** Steel – 43 wt% Cu showing continuous copper films, some of which crack

There is very good agreement between cracking susceptibility and microstructure. Micrographs of varying compositions are shown in Figures 4 through 7. Figure 4 shows the FZ and HAZ of a Steel – 63 wt% Cu sample. This falls within the region of low FZ cracking susceptibility at high copper concentrations. No cracks were observed in the FZ, it is believed, because enough copper was present to backfill any cracks that might have formed. However, there was Cu penetration along former austenite grain boundaries. This is representative of copper’s effect on the HAZ when terminal copper was observed in the FZ. Figure 5 is a Steel – 49 wt% Cu sample, which falls within the region of high FZ crack susceptibility. Cracking in the FZ appears to fall along regions of continuous copper, which appear as copper “rivers”. As the sample cooled, thermal contraction stresses increased to a point that the copper film was no longer able to support the stress. This is classical

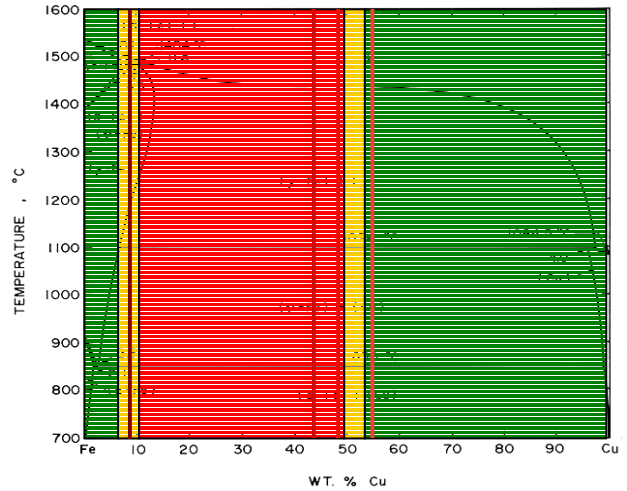


**Figure 3:** FZ Cracking susceptibility in Steel – Cu welds. green, Low; yellow, Moderate; red, High. Compositions of Figures 4-7 indicated

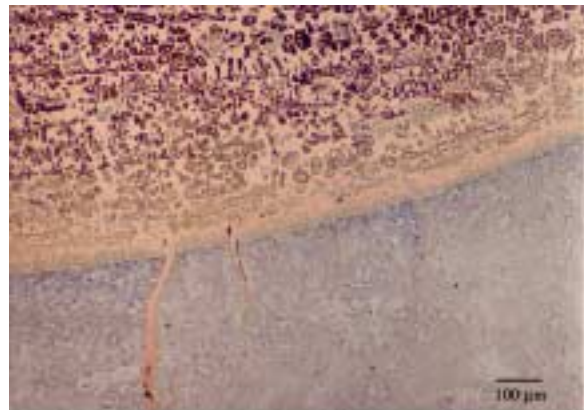


**Figure 4:** Steel – 63 wt% Cu. No cracking in FZ, but Cu penetration along prior  $\gamma$  grain boundaries

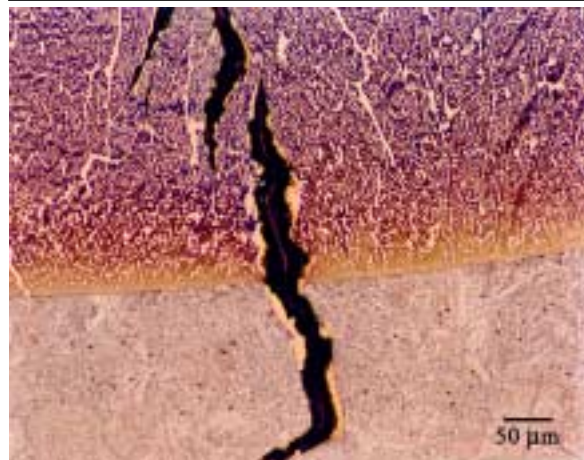


**Figure 5:** Steel – 49 wt% Cu. Crack in FZ extends into HAZ along prior  $\gamma$  grain boundary

solidification cracking. A Steel – 43 wt% Cu sample is shown in Figure 6. Cracking along continuous films of copper is easily seen. This falls well within the high crack susceptible region. Figure 7 is a Steel – 9.2 wt% Cu sample that falls at the lower composition cracking range, and within the moderate crack susceptible region. What is significant to note is the presence of copper appearing spheres on the order of one micron in diameter. These spheres were confirmed as copper by performing Energy Dispersive Spectroscopy using an EPMA in spot mode at 20 keV. The presence of these copper spheres at a composition less than the binary Fe-Cu peritectic isotherm maximum composition of Fe – 11.2 wt% Cu is not predicted by the equilibrium binary phase diagram. Their presence can be explained by any combination of three factors; 1) non-equilibrium solidification conditions, 2) ternary peritectic maximum copper composition that is less than 9.3 wt% copper and 3) composition determined by geometric dilution measurement was less than the actual composition. The simplest, and most probable given the high cooling rates associated with fusion welding, would be non-equilibrium solidification conditions.

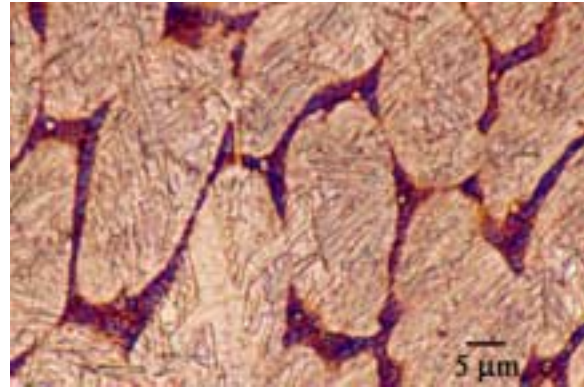


**Figure 7:** Steel – 9.2 wt% Cu. Small Cu spheres are seen in inter columnar region

### Solidification Modeling

In order to determine the solidification condition, the dimensionless back diffusion parameter  $\alpha$  was calculated following the Scheil (ref.) solidification model for the Steel – 7.2 wt% Cu sample. Diffusion data was obtained for copper in  $\delta$  ferrite (ref. Arita). Solidification time was estimated by using the Rosenthal (ref.) approximation to determine cooling rate and the binary Fe-Cu liquidus and solidus lines were used to determine the solidification temperature range (i.e. no liquid under cooling). Additionally, dendrite arm spacing measurements were obtained directly from the sample. The back diffusion parameter was calculated to be .00357, indicating that non-equilibrium, Scheil solidification conditions exist. It is believed that the presence of the copper spheres in the Steel – 9.2 wt% sample is a result of non-equilibrium solidification conditions.

Knowing the solidification conditions, the quantity of terminal copper can be modeled using the Scheil equations in conjunction with a finite difference technique (ref.?). To do this, the liquidus and solidus compositions were taken directly from the Fe-Cu phase diagram at each weight percent

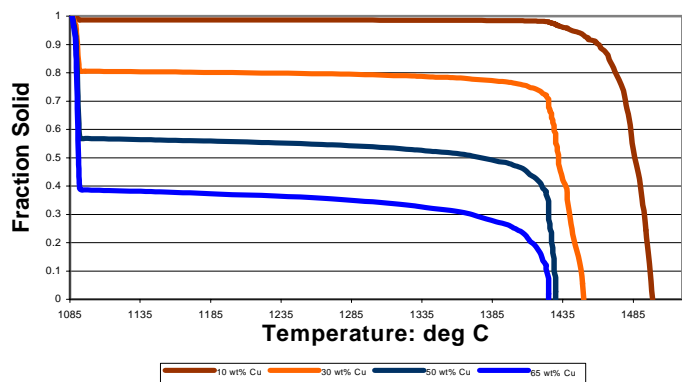


**Figure 8:** Fraction solid vs. Temperature using Scheil model for various compositions of Copper

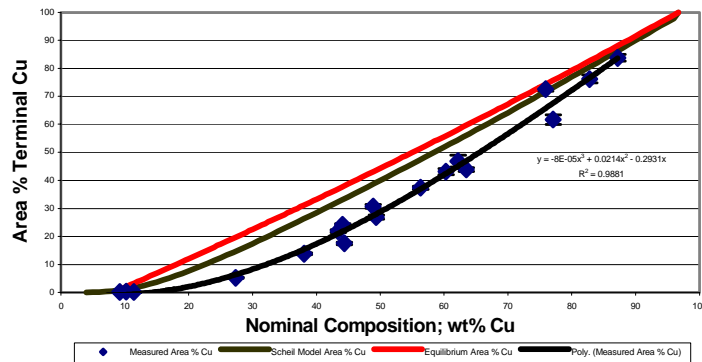


**Figure 9:** Area percent terminal copper versus nominal composition as predicted by Scheil and Equilibrium modeling, compared to measured values

equilibrium modeling used the Fe-Cu binary phase diagram for all data. The lever rule was used to determine the weight fraction of both the Fe rich and Cu rich phases at the Cu peritectic isotherm, 1096°C. Weight fraction was then converted to area percent by using knowing taking the average density of the Fe rich and Cu rich phases to be 7.96 and 8.96 g/cm<sup>3</sup> respectively. It was assumed that area fraction and volume fraction would be equal, thus allowing a comparison between cross sectioned samples and solidification models. QIA was used to measure area fraction terminal copper in each sample by evaluating twenty fields per sample, resulting in the data displayed in Figure 9. High cracking susceptibility occurs when volume percent terminal copper is between 0.14% - 43%.

In most situations, Scheil conditions will produce the greatest amount of terminal solute due to the absence of solid diffusion which does not allow the equilibrium solidus composition to be maintained throughout the solid with decreasing temperature. However, as seen in Figure 9, the equilibrium modeling predicts the greatest terminal solute. This is due to the decreasing copper concentration in austenite as Fe – Cu alloys cool. In the equilibrium case, diffusion of Cu in the solid would create a greater volume of terminal copper for any given nominal composition. However, in non-equilibrium Scheil conditions there is limited diffusion in the solid and the copper is retained in the solid matrix as the melt solidifies.

The measured values show relatively good agreement with the Scheil model with the noted exception that at any nominal composition, less terminal peritectic copper was observed than the Scheil model predicted. This can be attributed to the effects of alloying elements other than Fe and Cu which constitute the binary phase diagram used for this modeling. Carbon content greater than .03 wt% has been shown to form two liquid layers in Fe – Cu alloys (ref. Iwase). Furthermore, there are ??? elements in the Steel – Copper samples that may have a significant effect on the ability of the primary solid to absorb Copper.

copper from 1 to 100 wt%, resulting in a total of 200

measurements. The finite difference iterative technique using the Scheil equations was then used to predict the fraction solid vs. temperature for Steel – 10, 30, 50 and 65 wt% Copper as seen in Figure 8.

The Scheil model was then used to predict the volume percent terminal peritectic copper phase and compare that to both the equilibrium predictions and the actual measured values of area percent terminal peritectic. The

## Summary

A FGM of commercially pure copper into AISI H-13 tool steel was built using the LENS process. Solidification cracking and porosity were observed in the build. Dilution control experiments were carried out to determine the compositional cracking range of Copper in AISI 1013 steel, a representative system for H-13 tool steel. Cracking susceptibility was arranged into three categories; low, medium and high. Low susceptibility occurred from approximately 0- 8 wt% Cu and from – approximately 52.5 to 100 wt% Cu. Moderate susceptibility occurred from 8 – 11.5 wt% Cu and 50 - 52.5 wt% Cu and high susceptibility to cracking occurred from 11.5 – 50 wt% Cu with a corresponding volume fraction terminal copper ranging from 0.14% - 43%.

Sample Number	wt% Cu in FZ	Cracking		
		FZ Macro	FZ Cross Section	HAZ
1	7.2	none	none	none
2	8.9	none, steady	none	none
3	9.2	yes, center line	slight	yes
4	10.2	yes, center line	slight	slight
5	10.6	none	none	none
6	10.8	none	none	none
7	11.3	none, steady	none	slight
8	11.4	slight	slight	slight
9	12.9	none	none	slight
10	27.4	yes	yes	yes
11	38.1	yes	yes	yes
12	43.4	yes	yes	yes
13	44.1	slight, initially	yes	yes
14	44.4	none	no	slight
15	48.9	slight, initially	yes, center line	yes
16	49.4	none	yes, center line	yes
17	56.3	none	none	slight
18	60.3	none	none	yes
19	62.2	none	none	none
20	63.5	none	none	yes
21	75.9	none	none	yes
22	77.0	none	none	yes
23	82.8	none	none	yes
24	87.2	none	none	yes
25	87.7	none	none	slight
26	95.5	none	none	slight
27	96.8	none	none	slight
28	97.1	none	none	slight
29	97.7	none	none	slight

**Table 2 – Steel- Cu Dilution Control Experiment Compositions and Observations**